

Article

Fault Diagnosis for Body-in-White Welding Robot Based on Multi-Layer Belief Rule Base

Bang-Cheng Zhang^{1,2}, Ji-Dong Wang¹, Zhong Zheng^{1,*}, Dian-Xin Chen^{1,*} and Xiao-Jing Yin¹

¹ The School of Mechanical and Electrical Engineering, Changchun University of Technology, Changchun 130103, China; zhangbangcheng@ccut.edu.cn (B.-C.Z.); wangjidsun@163.com (J.-D.W.)

² The School of Mechanical and Electrical Engineering, Changchun Institute of Technology, Changchun 130103, China

* Correspondence: m18634233795@163.com (Z.Z.); cdx15764468016@163.com (D.-X.C.); Tel.: +86-18-6342-33795 (Z.Z.); +86-15-7644-68016 (D.-X.C.)

Abstract: Fault diagnosis for body-in-white (BIW) welding robots is important for ensuring the efficient production of the welding assembly line. As a result of the complex mechanism of the body-in-white welding robot, its strong correlation of components, and the many types of faults, it is difficult to establish a complete fault diagnosis model. Therefore, a fault diagnosis model for a BIW-welding robot based on a multi-layer belief rule base (BRB) was proposed. This model can effectively integrate monitoring data and expert knowledge to achieve an accurate fault diagnosis and facilitate traceability. First, according to the established fault tree, a fault mechanism was determined. Second, based on the multi-layer relationship of a fault tree, we established a multi-layer BRB model. Meanwhile, in order to improve the accuracy of the model parameters, the projection covariance matrix adaptive evolutionary strategy (P-CMA-ES) algorithm was used to optimize and update the parameters of the fault diagnosis model. Finally, the validity of the proposed model was verified by a simulation experiment for the BIW-welding robot.

Keywords: welding robot; belief rule base; fault tree; P-CMA-ES algorithm



Citation: Zhang, B.-C.; Wang, J.-D.; Zheng, Z.; Chen, D.-X.; Yin, X.-J. Fault Diagnosis for Body-in-White Welding Robot Based on Multi-Layer Belief Rule Base. *Appl. Sci.* **2023**, *13*, 4773. <https://doi.org/10.3390/app13084773>

Academic Editors: Marco Cocconcelli, Matteo Strozzi and Gianluca D'Elia

Received: 16 March 2023

Revised: 4 April 2023

Accepted: 7 April 2023

Published: 10 April 2023



Copyright: © 2023 by the authors. Licensee MDPI, Basel, Switzerland. This article is an open access article distributed under the terms and conditions of the Creative Commons Attribution (CC BY) license (<https://creativecommons.org/licenses/by/4.0/>).

1. Introduction

With the promotion of modern industrial intelligent manufacturing, the traditional artificial manufacturing industry has been turning to the development trend of modern automated production with robots as the main body. As a large and complex system, the body-in-white (BIW) welding robot is difficult to judge and detect because of the complexity of the control object and the variety of tasks it handles. Faults in the welding production process lead to the shutdown of the welding production line as well as untimely or imperfect equipment maintenance, etc., which directly affects the welding production efficiency and reduces the quality of the body-in-white. Due to the highly integrated, independent, and intelligent nature of body-in-white welding robots, it is very challenging to study their overall normal operation statuses. Once a part of the welding robot fails, the loss and damage caused are far greater than those for ordinary mechanical equipment; the failure may cause equipment downtime, causing economic losses for the enterprise, and personnel accidents, leading to more serious disasters. Therefore, it is meaningful to conduct fault diagnosis research on the robot [1]. However, the complexity, correlation, and uncertainty of the welding machine system make it very difficult to study the fault diagnosis of the welding machine. It has become a difficult problem to establish a fault diagnosis model for welding robots and to improve the diagnosis accuracy.

The BIW-welding robot is an integrated system containing mechanical, electrical, control, and other complex system components. The work object is complex, and the processing tasks are heavy, resulting in a high probability of failure. As a result, the research on its fault diagnosis has also received increasing attention from experts and

scholars at home and abroad. At present, there are mainly three types of fault diagnosis methods: analytical model-based methods [2], data-driven methods [3], and qualitative knowledge-based methods [4]. Behrouz et al. [5] proposed an adaptive order tracking method with a recursive Kalman filter algorithm to implement fault diagnosis on induction motors. Yang et al. [6] proposed an improved fuzzy hierarchical analysis method to realize the application of condenser fault diagnostics in power plants. The above analytical model can effectively and accurately determine the fault. However, the number of variables and influencing factors in the real environment makes it difficult to establish accurate mathematical and analytical expressions. Chen et al. [7] proposed a method based on the maximum overlap discrete wavelet transform and artificial neural networks to realize the fault diagnosis of a distributed generation system; Liu et al. [8] proposed a method combining feature vector selection and support vector machines to handle the question of classifying imbalanced data. Zheng et al. [9] proposed a hidden Markov model approach to achieve the application of ball mill gearbox fault diagnosis. The above methods have a powerful function for simulating the real system. However, in practice, a large amount of training data are often required to train the system model, and the training data often have the difficulty of a small sample size which is difficult to obtain. Most data-driven approaches are “black-box modeling”, leading to problems such as the lack of interpretability of diagnostic results. Guo et al. [10] proposed a VFDR fault diagnosis strategy based on expert knowledge to realize its application in variable refrigerant flow system fault diagnosis. Zheng et al. [11] proposed a fault tree and Bayesian-based approach to address applications in the fault diagnosis of overhead crane equipment. Hu et al. [12] proposed a robot joint fault diagnosis method based on a BP neural network, which could solve the problem of the low accuracy of robot joint fault diagnosis. The above methods can obtain better fault diagnosis results. However, the system structure is usually complex and lacks the ability to handle quantitative data.

In summary, there are some results of the current research on the problem of complex system fault diagnosis [13]. However, the BIW-welding robot is a complex production process with multiple processes and conditions, and its failure characteristics are numerous. It becomes very difficult to establish an accurate mathematical analysis model, and accurate results cannot be obtained by relying on qualitative knowledge. Only using data-driven methods lacks interpretability and cannot utilize the experience and knowledge of experts, and the above three methods lack the ability to deal with various types of uncertain information. Yang et al. [14–17] proposed a belief rule base (BRB) expert system based on an evidential reasoning approach that could handle uncertain information that arises in the human decision-making process. For uncertain information, BRB can express it at the same time and can combine the advantages of quantitative analysis and qualitative analysis to obtain credible fault diagnosis results while ensuring model accuracy. By using numerical data to optimize the initial parameters in the BRB model, the relationship between input and output could be more intuitively described. The initial parameters of the BRB model can be fine-tuned through expert knowledge, and the BRB model reasoning method is used in fault diagnosis, life evaluation, and other fields. Expert systems have the characteristics of multi-type information processing. In contrast to the above disadvantages, the BRB expert system has the ability to handle both the lack of data and conflicting evidence. When dealing with qualitative and quantitative information, the BRB expert-system learning model is an optimization problem with linear and nonlinear constrained optimization. Meanwhile, the BRB model is prone to the combinatorial explosion problem that affects the final results [18]. For the above-mentioned problems, the multi-layer BRB model can be used to solve them. The main idea of the multi-layer BRB is to adopt a bottom-up model. First, the underlying indicators and second, the use of the combination result are combined as the input of the next layer and finally reach the target state [19]. The advantage of multi-layer BRB over single-layer BRB is that the system is built according to the system structure. The multi-layer BRB hierarchy effectively reduces the number of rules and effectively avoids the combination explosion generated by the BRB model.

As a result, this paper uses a multi-layer BRB, a semi-quantitative tool, to construct a fault diagnosis model that incorporates expert knowledge and quantitative data. This model addresses the limitations of using only single knowledge for diagnosis by utilizing surveillance data and expert knowledge to produce a better diagnosis. Realizing the comprehensive utilization of the working mechanism, failure mechanism, and the data of the BIW welding and assembly robot can improve the accuracy of diagnosis. The local adjustment of model parameters by the (P-CMA-ES) algorithm [20] can reduce the limitations of expert knowledge. The validity of the method was verified by experiments.

2. Mechanism Analysis and Problem Description of BIW-Welding Robot

2.1. Mechanism Analysis and Fault Tree Construction of BIW-Welding Robot

At present, the BIW-welding robot is mainly used in the welding production line for the welding production of the automobile BIW. The welding system is mainly composed of a welding gun, welding clamp, welding power source, wire feeder, gun clearing mechanism, and other components. The welding system is the basic component order to complete the welding task. In the automatic welding production of BIW, long-term welding by welding robots causes problems such as the residual welding slag in the contact tip and wear of the motor. As a result, it affects the welding efficiency and the welding quality of the body-in-white. In order to ensure the safe and stable operation of the welding production, a gun cleaning mechanism can be used to maintain the gun regularly based on its working cycle and maintenance needs. It can ensure the normal delivery of welding gas, remove the adhesion of the welding slag, and ensure that the elongation length of the welding wire is appropriate. Additionally, the service life of the welding gun can be extended, and its related equipment can guarantee the safety and stability of the BIW welding process.

The welding system failure modes are shown in Table 1 below.

Table 1. Welding system failure mode.

Equipment Name	Failure Mode	Fault Cause	Fault Effect
Welding power supply	Welding system without current	Electronic and electrical components burned out	Welding cannot be performed
Wire feeder	No normal wire feeding	Wire feed drive motor failure	Arc break
Welding torch	Cannot be soldered	Poor contact of welding torch cable	Reduced welding efficiency
Welding pliers	Cannot be soldered	Electrode cap failure	Cannot finish welding
Gun cleaning mechanism	Low injection pressure and low flow rate of silicone nozzle	Controller failure	Welding slag clogging the torch tip

At present, the body-in-white welding robot is relatively mature, and its failure probability is generally low. Some possible failures may not appear in the factory log; the log is only a simple presentation of the failure category, and there is no distinction between the failures and contact for analysis. The events represent the state of the current component or system, including top events, basic events, intermediate events, etc.; logic gates represent the symbols of the logical relationship between events, including “or gate”, “and gate”, etc. The fault tree analysis of the body-in-white welding robot can deeply analyze the relationship between faults. This paper combines the events and related logical relations in the fault tree analysis (FTA) with the establishment of a knowledge base for the BRB expert system to create a fault tree model for welding robots.

The fault tree of the BIW-welding robot system is built based on the conditions of a stable factory environment, with no worker operation errors and a smooth external power supply. In order for the welding robot system to perform the welding work, the robot body and its related systems must be able to work normally; that is, any failure in any of the four subsystems of the welding robot causes the welding robot to fail in its normal welding work. Therefore, the fault of the welding robot system was selected as the top event of the fault tree. According to the top-down establishment process of the fault tree, starting with

the fault of the welding robot system as the top event, the overall fault tree of the welding robot can be listed. By establishing a fault tree model for the welding robot, the correlation between faults can be clearly represented to clearly understand the cause of the fault and the fault propagation process of the entire system. Through the detailed decomposition of the structure and detailed analysis of the working mechanism of the welding robot system, the overall fault tree of the welding robot is established, as shown in Figure 1.

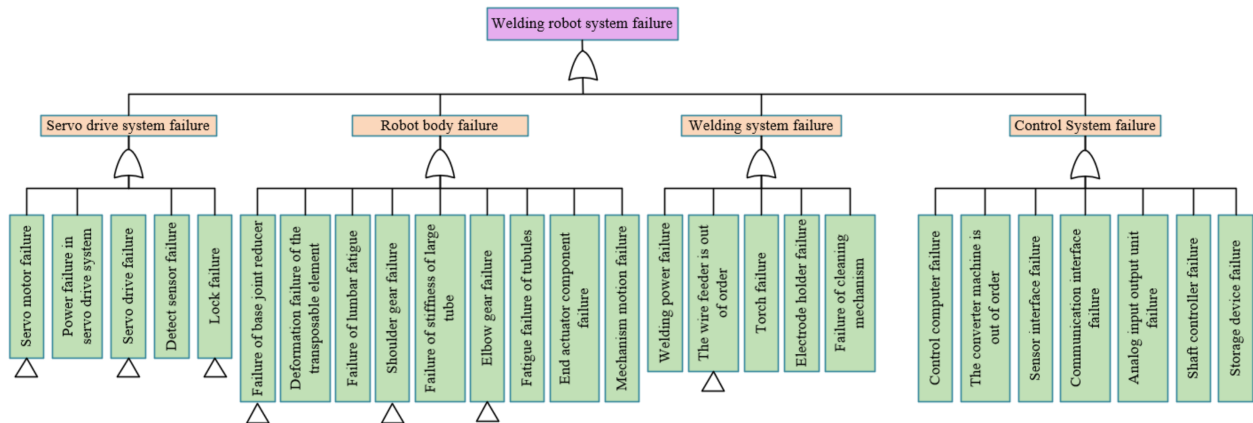


Figure 1. Welding robot system fault.

2.2. Problem Description of the Welding Robot

The components of the BIW-welding robot are complex and highly correlated, and the fault tree is used to decompose them layer by layer. The BIW-welding robot is more mature and less prone to failure. How to establish a complete fault diagnosis model to achieve the accurate diagnosis of the BIW-welding robot is a problem we attempted to solve in this paper.

3. Fault Diagnosis Method for BIW-Welding Robot Based on Multi-Layered BRB

3.1. Basic Knowledge of Multi-Layer BRB Model

The rules of BRB are usually determined by domain experts based on the empirical knowledge and historical data of the system model. Experts determine the initial values of important parameters of several rules with a belief distribution and embed expert knowledge into the rules to form a BRB. The multi-layer BRB system is composed of several sub-rule bases, each consisting of a certain number of rules. The basic structure of the rules is as follows:

$$R_k^e : \text{If } (x_1 \text{ is } H_1^k \wedge x_2 \text{ is } H_2^k \dots x_M \text{ is } H_M^k, \text{ then } y \text{ is } \{(D_1, \beta_{1,k}), (D_2, \beta_{2,k}) \dots (D_N, \beta_{N,k})\}, \text{ with rule } \theta_k, \text{ attribute weight } \delta_1, \delta_2, \dots, \delta_M \tag{1}$$

where $R_k^e (e = 1, 2, \dots, S)$ represents the Kth rule of the eth sub-rule base; x_i stands for the attribute input; H_i^k indicates the attribute input reference value ($i = 1, 2, \dots, M$), y represents the output result, as the input information for the next layer; D_i indicates the reference level of the output results; β_i indicates the belief level relative to the reference level ($j = 1, 2, \dots, N$); θ_k represents the rule weight and δ_k indicates the attribute weight.

The multi-layer BRB model is shown in Figure 2. If all the input attributes of the system are divided into n sub-rule bases, $x_i^j (i = 1, 2, \dots, l, j = 1, 2, \dots, m, \dots, n)$ is represented as the i-th attribute input in the j-th rule base BRBj ($j = 1, 2, \dots, m, \dots, n$), ($j = 1, 2, \dots, m, \dots, n$) represents the output at the jth rule base, and the output of the sub-rule base is used as the input to the next level rule base, which is iterated until state y_n is reached.

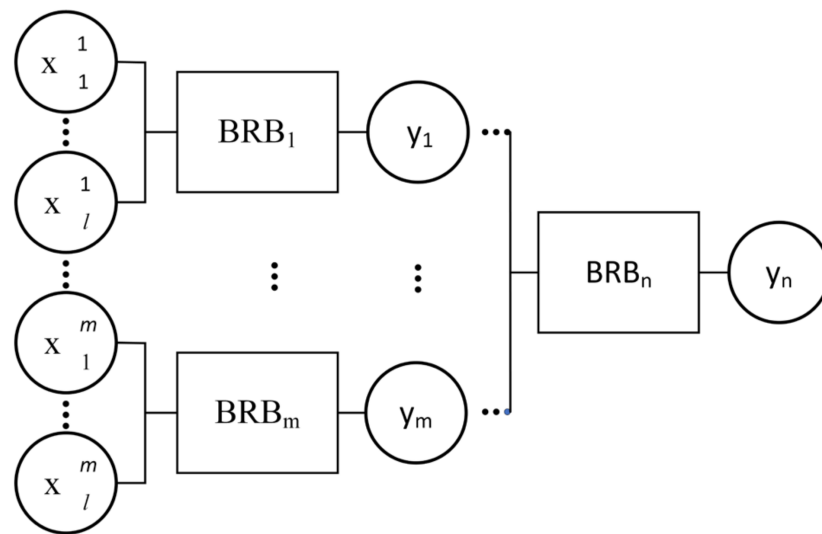


Figure 2. The basic structure of the multi-layer BRB model.

The multi-layer BRB model can deal with the problems of uncertainty and ambiguity more accurately through the reasoning and combination of multiple levels and propose higher reliability and precision of reasoning. The rule base and belief assignment function at each level can be interpreted and parsed, which is convenient for users to conduct model analysis and optimization. At the same time, layers can be added or deleted according to specific problem requirements and can more flexibly adapt to the application requirements of different scenarios.

3.2. Establishment of Multi-Layer BRB Diagnosis Model

Bayesian networks can be used to represent causal relationships between variables using directed acyclic graphs. In Figure 3, the logical relationships in the fault tree correspond to the Bayesian network. Parent nodes in Bayesian networks describe basic events in fault trees, and child nodes describe the top and middle events in the fault tree; conditional probabilities are used to describe the logical relationships constructed by the “with” and “or” gates.

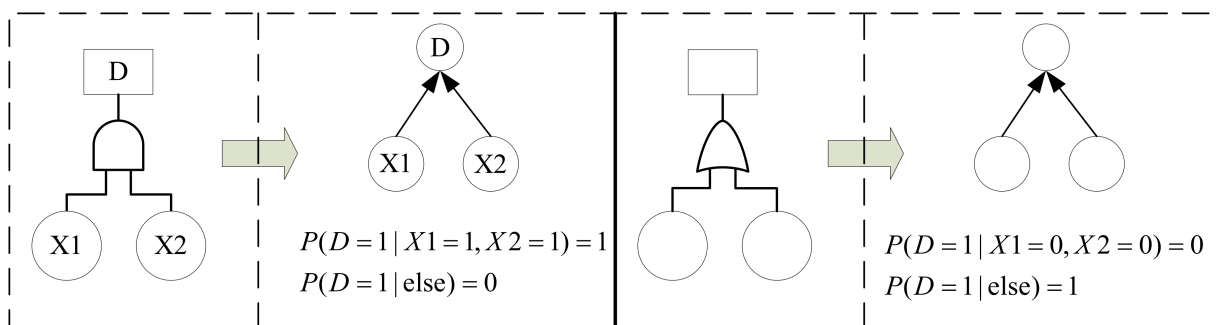


Figure 3. Transformation of fault trees and Bayesian networks.

In actual working conditions, the specific content of the fault description includes basic events and top events, which have different states. It can be supposed that the basic events X_1 and X_2 have two states: M_1 and M_2 states. They can be expressed as $A_{X1} = \{A_1, A_2, \dots, A_{M1}\}$ and $A_{X2} = \{A_1, A_2, \dots, A_{M2}\}$, respectively. The top event has a status that can be expressed as $\{D_1, D_2, \dots, D_N\}$. As shown in Figure 4, the parent and child nodes in the Bayesian network can be represented as:

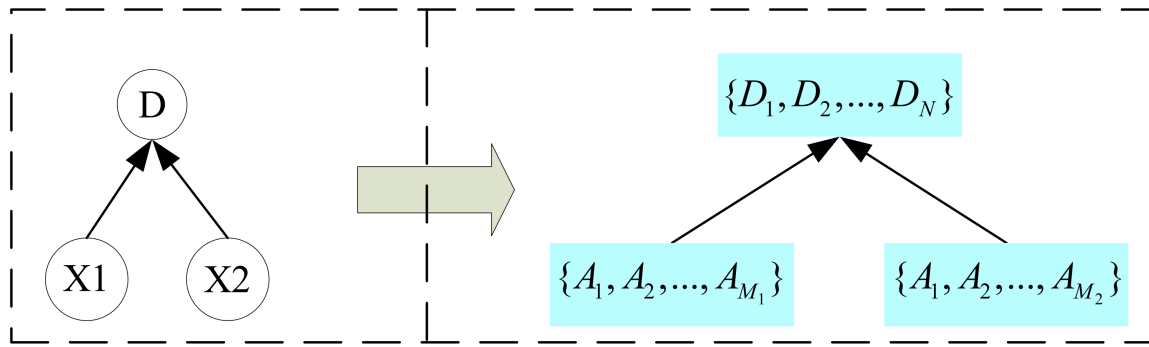


Figure 4. Node representation of Bayesian networks.

The conditional probability reasoning between parent and child nodes in Bayesian networks represents the nonlinear relationship between them. Combined with the construction process of the BRB network, the Bayesian network fragment in the above figure can be naturally converted into a BRB. The Kth rule in BRB can be expressed as:

$$R_k : \text{If } (X_1 \text{ is } A_1^k) \wedge (X_2 \text{ is } A_2^k), \text{ then } \{(D_1, \beta_{1,k}), (D_2, \beta_{2,k}) \dots (D_N, \beta_{N,k})\}, \quad (2)$$

with a rule weight θ_k ($k = 1, 2, \dots, L$) and attribute weight $\delta_{k1}, \delta_{k2}, \dots, \delta_{kT_k}$

where the reference values of prerequisite attributes X_1 and X_2 are $A_{X1} = \{A_1, A_2, \dots, A_{M1}\}$ and $A_{X2} = \{A_1, A_2, \dots, A_{M2}\}$, respectively.

Figure 5 shows an example of a fault tree for a welding robot. Combined with the multi-layer model, this can be divided into two layers and five sub-rule base systems, where the inputs of the first four sub-rule bases are the corresponding failure faults of each system component, and the inputs of the first four sub-rule bases are the outputs for the fifth sub-rule base. Sub-rule base five is the first layer of the welding robot fault diagnosis model. Meanwhile, it can diagnose the body’s welding robot system. The second level is to diagnose each component in the servo drive system failure, including the robot body failure, welding system failure, and control system failure, respectively. It is divided into four sub-rule bases in total, and the welding robot diagnosis model based on multi-layer BRB is established by using the expert’s experience, knowledge, and input monitoring quantity. The model can judge the fault of the welding robot system by inputting the monitoring quantity. Compared with the single-layer BRB, the established multi-layer BRB effectively avoids the problems of the combination explosion and parameter optimization caused by the BRB model.

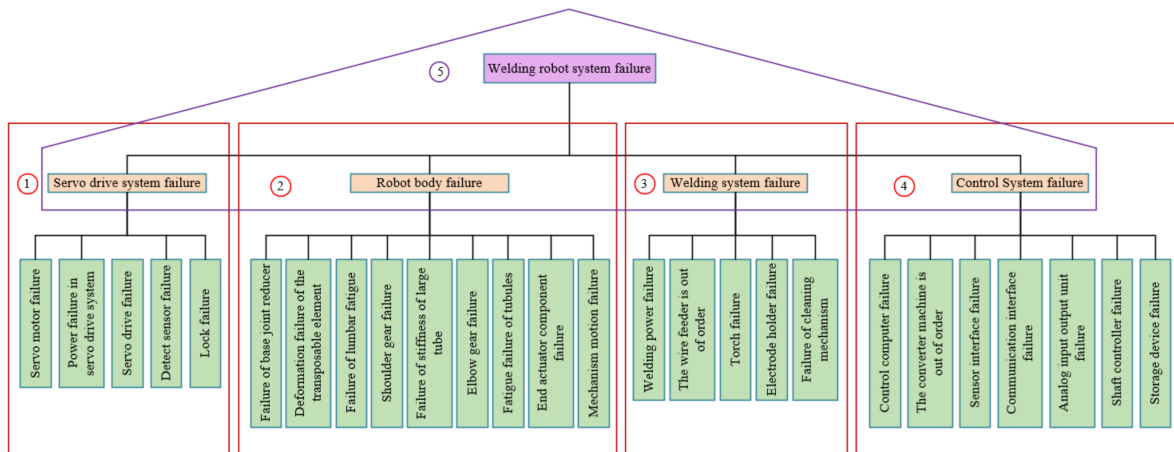


Figure 5. Multi-layer BRB model for diagnosis of welding robot systems.

3.3. Reasoning and Optimization Based on Multi-Layered BRB Fault Diagnosis Model

3.3.1. Model Reasoning

When the input feature parameters reach the BRB model, the reasoning of the model is mainly realized through the evidence reasoning (ER) algorithm. The specific steps for this are as follows:

1. The matching degree of the input reference value can be found:

$$\begin{aligned} \alpha_i^k &= \frac{A_i^{l+1} - X_i}{A_i^{l+1} - A_i^l} \quad k = l(A_i^l \leq X_i \leq A_i^{l+1}) \\ \alpha_i^k &= 1 - \alpha_i^k \quad k = k + 1 \\ \alpha_i^k &= 0 \quad k = 1, \dots, N(k \neq l, l + 1) \end{aligned} \tag{3}$$

where a_i^k denotes the match of the reference value A_i for the i th input X_i .

2. Calculation of activation weights The main logic gates used in the FTA are the "with" and "or" gates, so the rules are activated and calculated according to the conversion rules.
3. ER inference algorithm The belief level of each evaluation result is generated using the ER inference algorithm with the following expressions:

$$\hat{\beta}_n = \frac{\mu \times \left[\prod_{k=1}^L \left(\omega_k \beta_{n,k} + 1 - \omega_k \sum_{n=1}^N \beta_{n,k} \right) - \prod_{k=1}^L \left(1 - \omega_k \sum_{n=1}^N \beta_{n,k} \right) \right]}{1 - \mu \times \left[\prod_{k=1}^L (1 - \omega_k) \right]} \tag{4}$$

4. Output results The final output of the BRB model reasoned by the ER algorithm is:

$$output = \sum_{n=1}^N D_n \beta_n \tag{5}$$

3.3.2. Parameter Optimization of the Model

The initial parameters of the BRB model are given according to expert experience and expert knowledge. However, the limitations of the expert's knowledge on the expertise can make the given parameters inaccurate. In this paper, the Projection Covariance Matrix Adaption Evolution Strategy (P-CMA-ES) algorithm with projection operation was used to optimize the parameters of the fault diagnosis model for updating.

The constraints on the BRB model parameter vector $V = [\theta^1, \dots, \theta^k, \dots, \delta^1, \dots, \delta^m, \beta_1^k, \dots, \beta_n^k]^T$ were:

$$\min MSE(y(\theta^k, \delta^m, \beta_n^k)) \tag{6}$$

$$\begin{aligned} s.t. \quad & 0 \leq \theta_k \leq 1 \\ & 0 \leq \beta_{n,k} \leq 1, n = 1, 2, \dots, N \\ & \sum_{n=1}^N \beta_{n,k} \leq 1, k = 1, 2, \dots, L \\ & 0 \leq \delta_i \leq 1, i = 1, 2, \dots, M \end{aligned} \tag{7}$$

The objective function was:

$$MSE = \frac{1}{T} \sum_{i=1}^T (y_i - y_{ir})^2 \tag{8}$$

where $MSE(y(\theta^k, \delta^m, \beta_n^k))$ is the mean squared error (MSE), T is the amount of data and y_{ir} is the true semantic value.

The specific steps of the P-CMA-ES algorithm are as follows:

1. Initial value setting.

Set the initial parameters $x^0, C^0, \sigma, g, \lambda$, respectively, to refer to the initial parameter vector, initial covariance matrix, initial step size, evolutionary algebra, and population size.

2. Generate initial populations.

$$X_k^{g+1} \sim m^g + \sigma^g \mathbb{N}(0, C^g), \text{ for } k = 1, \dots, \sim \tag{9}$$

3. Project the solution to the feasible region.

$$X_i^{g+1}(1 + n_e \times (j - 1) : n_e \times j) = X_i^{g+1}(1 + n_e \times (j - 1) : n_e \times j) \Psi - \Psi_e^T \times (\Psi_e \times \Psi_e^T) \times X_i^{g+1}(1 + n_e \times (j - 1) : n_e \times j) \times \Psi_e \tag{10}$$

4. Selection and reorganization.

$$m^{g+1} = \sum_{i=1}^{\mu} \omega_i X_{i:\lambda}^{g+1} \tag{11}$$

5. Update the overall covariance matrix

$$C^{g+1} = (1 - c_1 - c_2) C^g + a_1 p_c^{g+1} (p_c^{g+1})^T + c_2 \sum_{i=1}^{\varepsilon} \gamma_i \left(\frac{(X_{1:\lambda}^{g+1} - \text{mean}^g)}{\eta^g} \right) \left(\frac{(X_{1:\lambda}^{g+1} - \text{mean}^g)}{\eta^g} \right)^T \tag{12}$$

6. Repeat the above operations until the optimal solution is obtained.

The model parameters are optimized and updated through this algorithm. The advantage of this algorithm is that it reduces the complexity of the algorithm, thus improving the effectiveness of optimization.

4. Case Studies

This article uses the statement that “the attitude and suspension height of the welding gun is wrong” to explain the realization process of the fault diagnosis of the body welding robot. Based on previous analysis, the BIW-welding robot has a complex structure, and there are many reasons for its failure. However, with the continuous iteration of technology, welding robots are becoming more mature, and their probability of failure is gradually decreasing. The performance of parts of the BIW-welding robot gradually degrades with the operation of the welding production process until it fails. When a fault occurs, the staff will repair and replace the faulty parts and record them in the corresponding logs, which can be filtered and organized to obtain the fault samples. Based on the fault samples, it is possible to use FTA and BRB to build a multi-layer fault diagnosis model for BIW-welding robots. In this paper, the fault data set was determined by the fault log data of a certain factory, the software simulated fault probability, and 100 sets of data relating to the fault diagnosis of the body-in-white welding robot were obtained, which established a fault tree of the welding robot system using the FTA-based method. The obtained data are shown in Figure 6. Among them, the data indicators used include drive power failure, a low power supply voltage, motor encoder failure, bearing wear failure, rotor permanent magnet demagnetization, a welding seam detection sensor failure, welding torch suspension height sensor failure, a welding torch suspension height sensor failure, the control computer failure, incorrect settings, and the incorrect settings for torch attitude and levitation height.

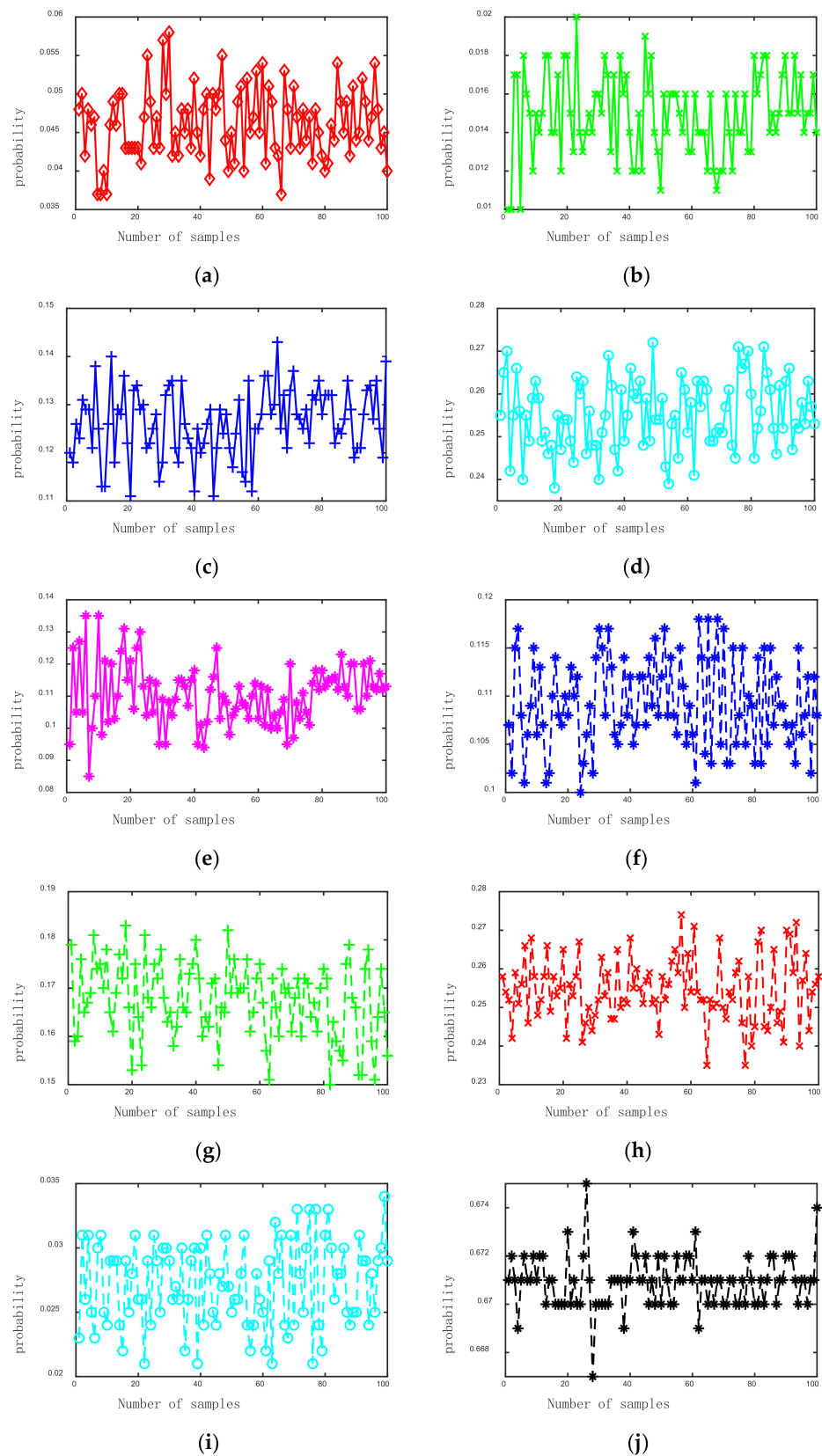


Figure 6. Experimental data. (a) Drive power failure; (b) The supply voltage is too low; (c) Motor encoder fault; (d) Bearing wear failure; (e) Demagnetization of rotor permanent magnet; (f) Weld detection sensor failure; (g) Welding gun suspension height sensor fault; (h) Control computer failure; (i) Setting error; (j) Incorrect setting of welding gun attitude and suspension height.

In building the fault diagnosis model for welding robots, the FTA was used to build a fault in the welding robot. The above conversion process was first used to transform it into a multi-layer BRB, and then the implementation process for the multi-layer BRB fault diagnosis model. This conversion process is shown in Figure 7.

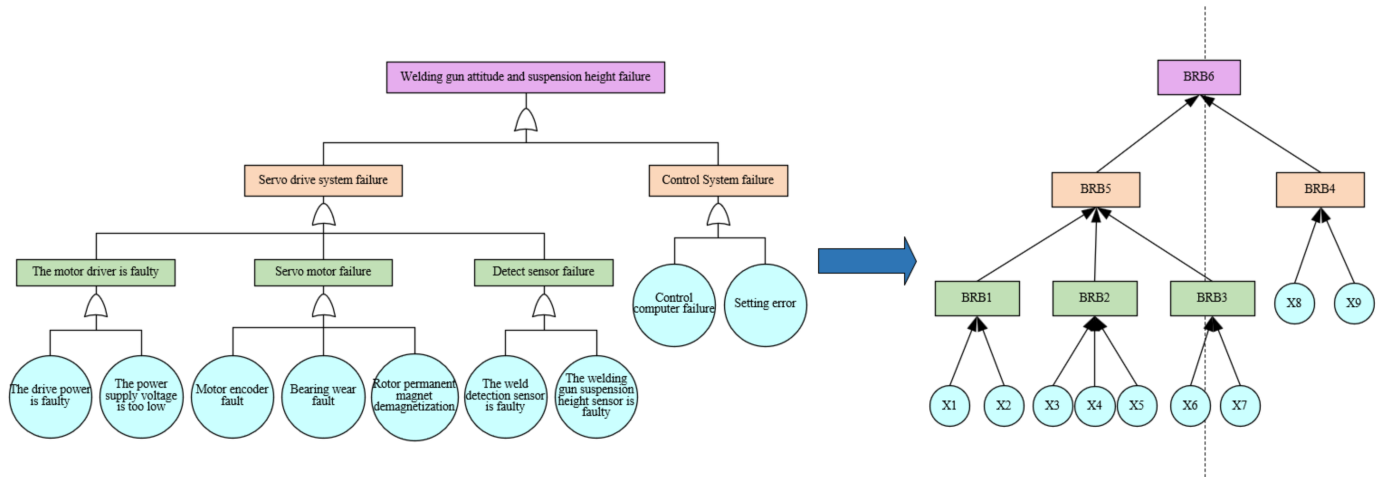


Figure 7. FTA to BRB conversion.

By observing the transformed BRB model, we can see that it has many attributes and a complex structure. In order to prevent problems such as combination explosion in BRB, a multi-layer BRB model was established, and the fault tree was divided into six sub-fault trees and transformed into a multi-layer BRB. In this section, the servo motor driver failure, the wrong torch attitude, and suspension height were used as examples for specific analysis. They correspond to the first sub-rule base and the sixth sub-rule base in the multi-layer BRB, namely BRB1, and BRB6. In BRB1, the two attributes of the drive power failure and supply voltage are too low and are represented by X_1 and X_2 , respectively. The belief rules of the BRB1-based fault diagnosis sub-model for the BIW-welding robot can be described as:

$$R_k : \text{If } (X_1 \text{ is } A_1^k) \vee (X_2 \text{ is } A_2^k), \text{ then } \{(D_1, \beta_{1,k}), \dots, (D_n, \beta_{n,k})\}, \quad (13)$$

with a rule weight θ_k ($k = 1, 2, \dots, L$) and attribute weight δ_{k1}, δ_{k2}

In BIW-welding robotic systems, the performance of the system and its components gradually decrease with time until failure occurs. The collected data usually have a certain distribution pattern. In the BRB model, the premise attribute reference value directly determines the distribution of the input data and also determines the number of belief rules in the model and the accuracy of model reasoning. As a result, this study set the reference value of the premise attribute based on data fluctuation and a level of uniform distribution. Then, the reference values and initial parameters of the BRB were determined according to the analysis results, and the input reference values of the BRB were selected using the method as described above. X_1 and X_2 set four reference levels, respectively, including small (S), medium (M), large (L), and very large (VL). The reference values of BRB1 are shown in Tables 2 and 3. Four reference levels were set for the servo drive system failure and control system failure: small (S), medium (M), large (L), and very large (VL). The reference values of BRB6 are shown in Tables 4 and 5.

Table 2. X_1 Reference values in BRB1.

S	M	L	VL
0.04	0.043	0.046	0.048

Table 3. X_2 Reference values in BRB1.

S	M	L	VL
0.01	0.012	0.014	0.016

Table 4. Fault reference value of servo drive system in BRB6.

S	M	L	VL
0.04	0.043	0.046	0.048

Table 5. Control system fault reference value in BRB6.

S	M	L	VL
0.272	0.277	0.282	0.286

According to the above setting of the reference level and reference value, a BIW-welding robot fault diagnosis model was established. The BRB1 model contains 16 belief rules, and the BRB6 model contains 16 belief rules. The cumulative sum can be set to one to obtain the initial fault diagnosis model. Tables 6 and 7 in the figure below show the initial parameters of the BRB1 model and the BRB6 model, respectively. The number of iterations for the P-CMA-ES algorithm can be set to 100, and the output results of the BRB1 and BRB6 models are shown in Figures 8 and 9.

Table 6. Initial parameters of BRB1.

Rule	Rule Weight	Input	Result
1	1	S \wedge S	(1 0 0 0)
2	1	S \wedge M	(0.8 0.1 0.1 0)
3	1	S \wedge L	(0.5 0.4 0 0.1)
4	1	S \wedge VL	(0.4 0.5 0 0.1)
5	1	M \wedge S	(0.3 0.6 0.1 0)
6	1	M \wedge M	(0.9 0 0.1 0)
7	1	M \wedge L	(0.8 0.2 0 0)
8	1	M \wedge VL	(0.5 0.4 0 0.1)
9	1	L \wedge S	(0.4 0.5 0 0.1)
10	1	L \wedge M	(0.2 0.7 0 0.1)
11	1	L \wedge L	(0.5 0.4 0 0.1)
12	1	L \wedge VL	(0.2 0.35 0.3 0.15)
13	1	VL \wedge S	(0.4 0.4 0.1 0.1)
14	1	VL \wedge M	(0.4 0.4 0 0.2)
15	1	VL \wedge L	(0.2 0.0.4 0.3 0.1)
16	1	VL \wedge VL	(0.1 0.5 0.3 0.1)

Table 7. Initial parameters of BRB6.

Rule	Rule Weight	Input	Result
1	1	S \wedge S	(1 0 0 0)
2	1	S \wedge M	(0.75 0.1 0.15 0)
3	1	S \wedge L	(0.4 0.4 0.1 0.1)
4	1	S \wedge VL	(0.4 0.4 0 0.2)
5	1	M \wedge S	(0.2 0.6 0.2 0)
6	1	M \wedge M	(0.8 0 0.1 0.1)

Table 7. Cont.

Rule	Rule Weight	Input	Result
7	1	M \wedge L	(0.7 0.2 0.1 0)
8	1	M \wedge VL	(0.4 0.4 0 0.2)
9	1	L \wedge S	(0.3 0.6 0 0.1)
10	1	L \wedge M	(0.2 0.6 0.1 0.1)
11	1	L \wedge L	(0.4 0.4 0 0.2)
12	1	L \wedge VL	(0.2 0.15 0.5 0.15)
13	1	VL \wedge S	(0.2 0.4 0.3 0.1)
14	1	VL \wedge M	(0.3 0.4 0 0.3)
15	1	VL \wedge L	(0.2 0.2 0.5 0.1)
16	1	VL \wedge VL	(0.2 0.4 0.3 0.1)

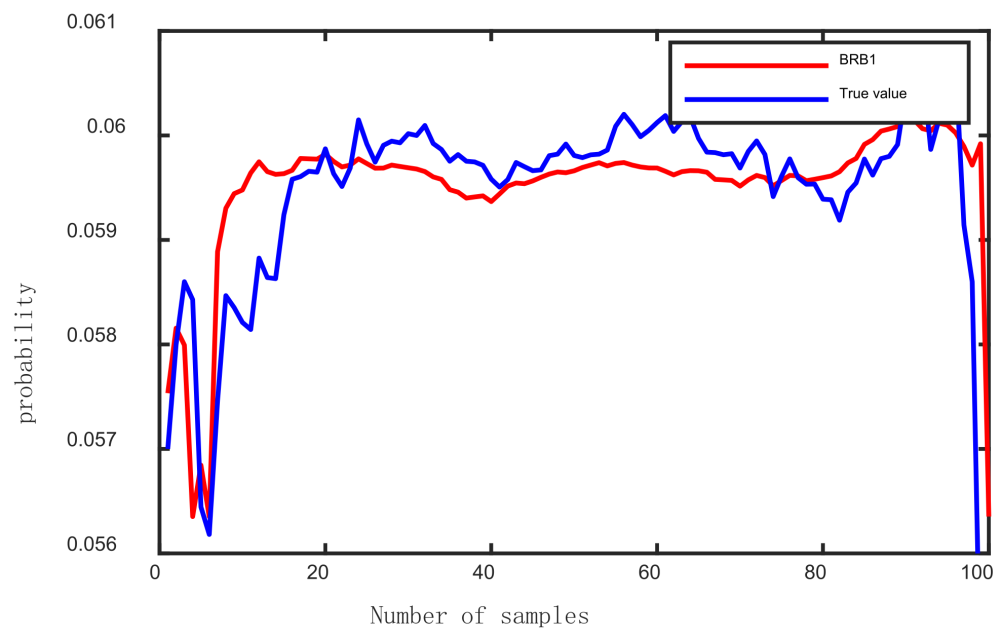


Figure 8. BRB1 output results.

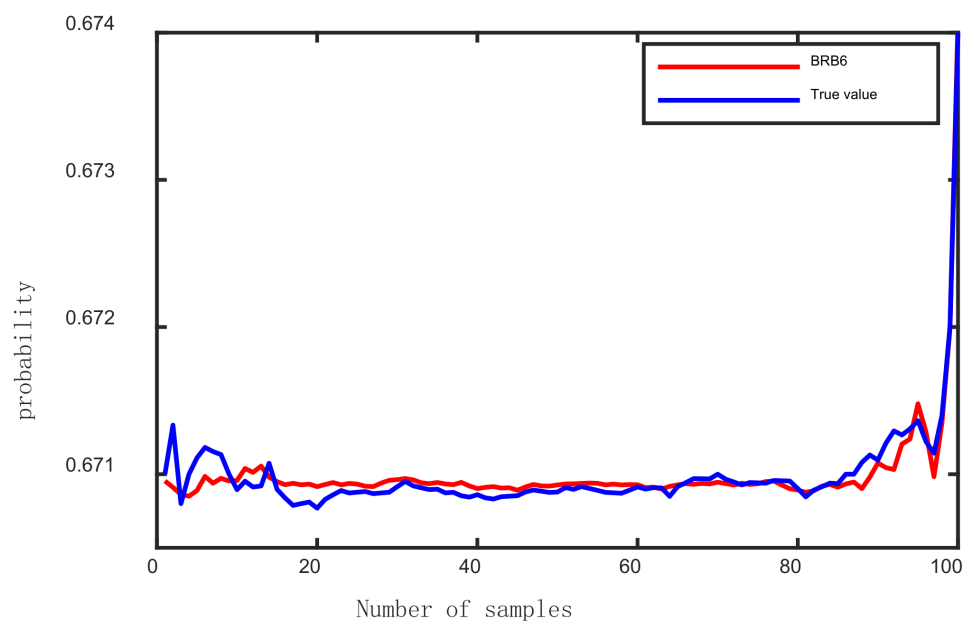


Figure 9. BRB6 output results.

Analyzing the output results of BRB1 and BRB6 showed that the MSE of the BRB1 model was 5.385×10^{-7} , and the MSE of the BRB6 model was 8.598×10^{-9} . The output of the model in this paper was found to fit the real values of torch attitude and suspension height failure well, which also proved the advantage of the model numerically.

In order to further verify the effectiveness of the proposed method in the BIW-welding robot fault diagnosis, a comparative experiment was conducted to compare with other modeling methods. Currently, commonly used fault diagnosis methods include fuzzy C-means clustering (FCM), the BP neural network, and RBF neural network, so this model can be compared with these three methods for verification. The data adopt the above 100 sets of fitted welding torch attitude and the true value of the suspension height fault. The comparison graph is shown in Figure 10. For comparison, the evaluation results of several methods and the mean square error (MSE) of each method were calculated. MSE is a common comparison method of the “average error”. The value of MSE can provide a measure of the quality of a model. Finally, the mean square error (MSE) can be used as a judgment criterion for the fault diagnosis model to evaluate the fault diagnosis of the BIW-welding robot.

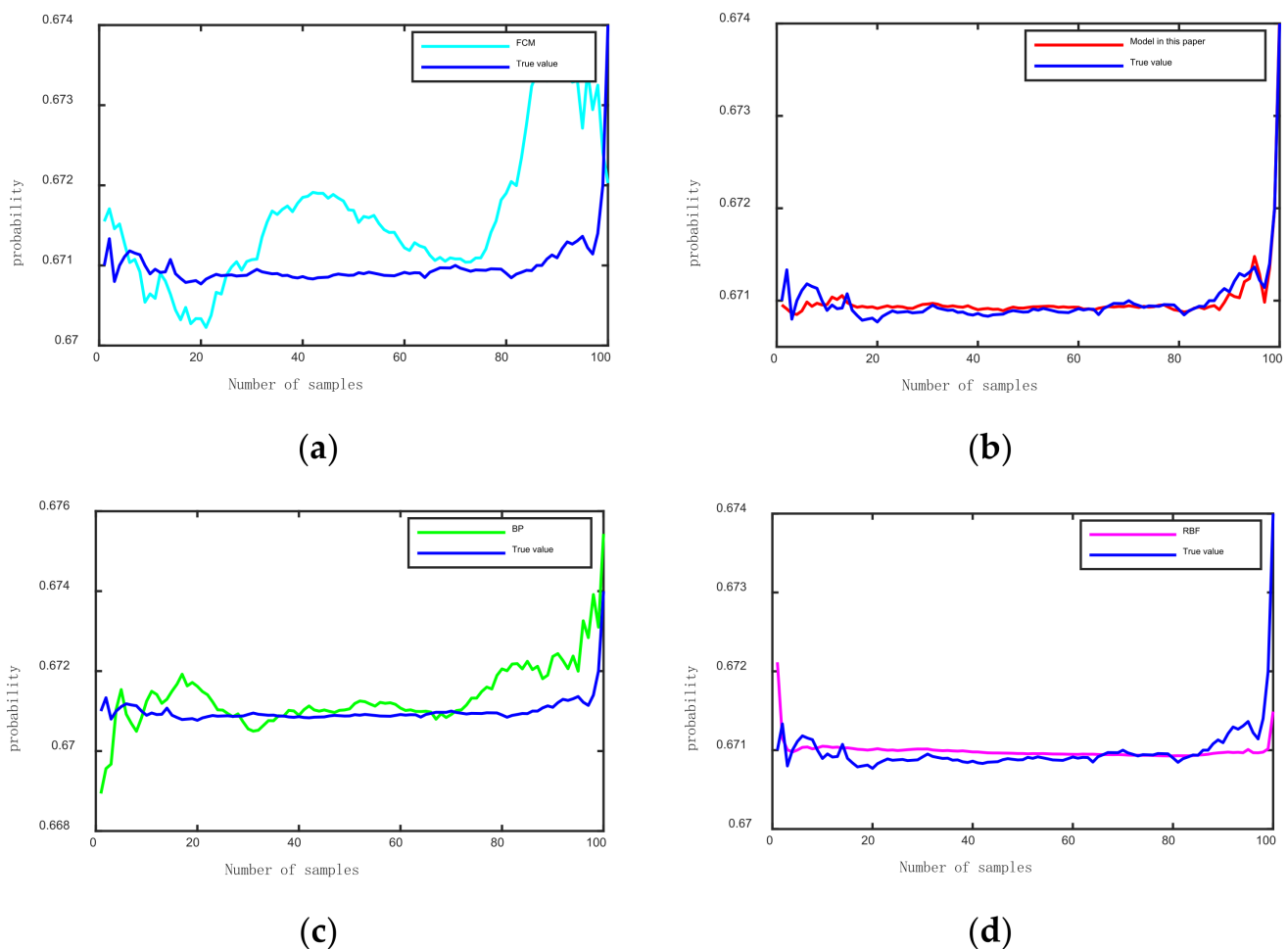


Figure 10. Comparison of this model with other methods. (a) Comparison chart of FCM method and real value. (b) The comparison chart of the model and the real value in this paper. (c) Comparison chart of BP neural network and real value. (d) Comparison chart of RBF method and real value.

The specific mean square error value is shown in Figure 11 below.

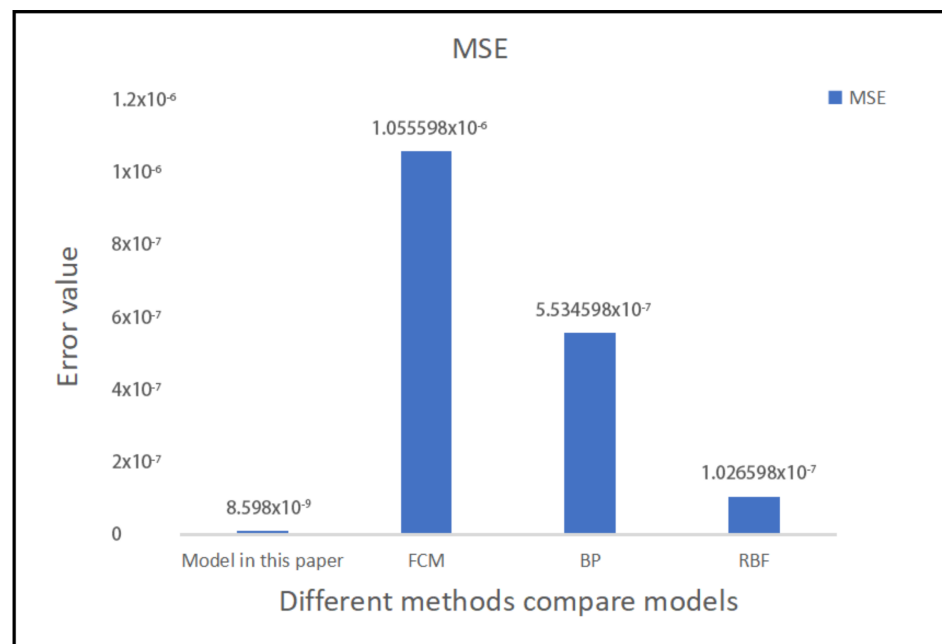


Figure 11. Comparison of mean square error of different methods.

The curve trend of each fault diagnosis model can be seen in Figure 10, in which the blue curve represents the real value, while the other color curves represent the trend curve obtained through different fault diagnosis models. It can also be seen that the curve trend of the model in this paper and the real data have the best-fitting effect. The RBF neural network is slightly less effective than this model, and the curve has the same trend as the data as a whole. The effect of the BP neural network is not good, and the curve is only partly similar to the trend of the data. The fuzzy C-means clustering (FCM) curve fluctuates significantly, and it is difficult to express a good diagnostic effect. Meanwhile, Figure 11 illustrates the validity of the above analysis in terms of data. According to Figure 11, it can be seen that the MSE of the model in this paper reached a minimum value of 8.598×10^{-9} , while the MSE of FCM was 1.055598×10^{-6} , the MSE of a BP neural network was 5.534598×10^{-7} , and the MSE of the RBF neural network was 1.026598×10^{-7} . The results obtained in Figures 10 and 11 are consistent, illustrating the validity of the model.

The model can be trained by combining testing data and expert knowledge and has a high training accuracy. At the same time, the effectiveness of the method in this paper was verified under the conditions of a complex structure and mechanism and difficult data acquisition. We can assume that the simulated data used in this paper were completely reliable. However, in actual working conditions, there were still deviations in the data we obtained, which may be due to the inaccurate data caused by the quality of the sensor. This situation affects the reliability of the data we use. Therefore, multi-level BRB models considering data reliability need further research. Additionally, future work may have better engineering implications.

5. Conclusions

This paper proposes a multi-layer BRB model for the fault diagnosis of body-in-white welding robots. This model can improve the fault diagnosis accuracy for a welding robot. In the proposed method, the multi-layer BRB model was constructed by transforming the results into BRB belief rules through the fault tree analysis of the BIW-welding robot. Meanwhile, updating and optimizing the model parameters through the P-CMA-ES algorithm can ameliorate the interference of some other factors with the model diagnosis results. This model can be applied to the fault diagnosis of welding robots, and the results show that, when compared with other models, it has a better diagnostic effect.

The model can make the results more reliable than traditional single-expert knowledge by utilizing the fusion of data and experience. Through the combination of the fault tree and multi-layer BRB model, the efficient diagnosis of other complex equipment can be realized.

Author Contributions: Conceptualization, B.-C.Z.; Methodology, D.-X.C. and X.-J.Y.; Software, J.-D.W.; Validation, Z.Z. All authors have read and agreed to the published version of the manuscript.

Funding: The research was supported by the Jilin Provincial Science and Technology Development Project under grants 20210301033GX, 20210201050GX, 20200401114GX, and 20200301038RQ.

Informed Consent Statement: Informed consent was obtained from all subjects for this study.

Data Availability Statement: The data used in this article are inconvenient to declare.

Conflicts of Interest: The authors declare no conflict of interest.

References

1. Nath, A.G.; Udmale, S.S.; Singh, S.K. Role of artificial intelligence in rotor fault diagnosis: A comprehensive review. *Artif. Intell. Rev.* **2020**, *54*, 2609–2668. [[CrossRef](#)]
2. Lu, C.; Tao, L.; Fan, H. An intelligent approach to machine component health prognostics by utilizing only truncated histories. *Mech. Syst. Signal Process* **2013**, *42*, 300–313. [[CrossRef](#)]
3. Lu, L.; Yan, J.; Meng, Y. Dynamic Genetic Algorithm-based Feature Selection Scheme for Machine Health Prognostics. *Procedia CIRP* **2016**, *56*, 316–320. [[CrossRef](#)]
4. Yu, J. Machine health prognostics using the Bayesian-inference-based probabilistic indication and high-order particle filtering framework. *J. Sound Vib.* **2015**, *358*, 97–110. [[CrossRef](#)]
5. Safarinejadian, B.; Zarei, J.; Ramezani, A. Fault Diagnosis of Induction Motors Using a Recursive Kalman Filtering Algorithm. *Int. Rev. Electr. Eng. IREE* **2013**, *8*, 96–103.
6. Yang, J.M.; Jia, Y.Q.; Liang, F.Y. The Application of Improved Fuzzy Analytic Hierarchy Process (FAHP) in the Condenser Fault Diagnosis. *Appl. Mech. Mater.* **2013**, *446*, 1104–1108. [[CrossRef](#)]
7. Chen, J.; Gao, J.; Jin, Y.; Zhu, P.; Zhang, Q. Fault Diagnosis in Distributed Power-Generation Systems Using Wavelet Based Artificial Neural Network. *Eur. J. Electr. Eng.* **2021**, *23*, 53–59. [[CrossRef](#)]
8. Liu, J.; Zio, E. Integration of feature vector selection and support vector machine for classification of imbalanced data. *Appl. Soft Comput.* **2018**, *75*, 702–711. [[CrossRef](#)]
9. Zheng, R.S.; Dong, X.M.; Hao, W.S.; Li, Y.; Wang, R.X. Application of Hidden Markov Models in Ball Mill Gearbox for Fault Diagnosis. *Adv. Mater. Res.* **2013**, *842*, 401–404. [[CrossRef](#)]
10. Guo, Y.; Wang, J.; Chen, H.; Li, G.; Huang, R.; Yuan, Y.; Ahmad, T.; Sun, S. An expert rule-based fault diagnosis strategy for variable refrigerant flow air conditioning systems. *Appl. Therm. Eng.* **2018**, *149*, 1223–1235. [[CrossRef](#)]
11. Zheng, Y.; Zhao, F.; Wang, Z. Fault diagnosis system of bridge crane equipment based on fault tree and Bayesian network. *Int. J. Adv. Manuf. Technol.* **2019**, *105*, 3605–3618. [[CrossRef](#)]
12. Hu, M.; Wu, J.; Yang, J.; Zhang, L.; Yang, F. Fault diagnosis of robot joint based on BP neural network. *Robotica* **2022**, *40*, 4388–4404. [[CrossRef](#)]
13. Yang, J.-B.; Liu, J.; Wang, J.; Sii, H.-S.; Wang, H.-W. Belief rule-base inference methodology using the evidential reasoning Approach-RIMER. *IEEE Trans. Syst. Man Cybern. Part A Syst. Humans* **2006**, *36*, 266–285. [[CrossRef](#)]
14. Yang, J.; Wang, Y.; Xu, D.; Chin, K. The evidential reasoning approach for MADA under both probabilistic and fuzzy uncertainties. *Eur. J. Oper. Res.* **2006**, *171*, 309–343. [[CrossRef](#)]
15. Yang, J.-B. Rule and utility based evidential reasoning approach for multiattribute decision analysis under uncertainties. *Eur. J. Oper. Res.* **2001**, *131*, 31–61. [[CrossRef](#)]
16. Huang, T.; Zhang, Q.; Tang, X.; Zhao, S.; Lu, X. A novel fault diagnosis method based on CNN and LSTM and its application in fault diagnosis for complex systems. *Artif. Intell. Rev.* **2021**, *55*, 1289–1315. [[CrossRef](#)]
17. Yang, J.-B.; Xu, D.-L. Evidential reasoning rule for evidence combination. *Artif. Intell.* **2013**, *205*, 1–29. [[CrossRef](#)]
18. Yin, X.; Wang, Z.; Zhang, B.; Zhou, Z.; Feng, Z.; Hu, G.; Wei, H. A Double Layer BRB Model for Health Prognostics in Complex Electromechanical System. *IEEE Access* **2017**, *5*, 23833–23847. [[CrossRef](#)]
19. Yang, J.-B.; Wang, Y.-M.; Xu, D.-L.; Chin, K.-S.; Chatton, L. Belief rule-based methodology for mapping consumer preferences and setting product targets. *Expert Syst. Appl.* **2012**, *39*, 4749–4759. [[CrossRef](#)]
20. Peng, S. *Research on Health State Prediction Method of Aero-Engine Gas Path System Based on Multi-Characteristic Quantity*; Changchun University of Technology: Changchun, China, 2022.

Disclaimer/Publisher's Note: The statements, opinions and data contained in all publications are solely those of the individual author(s) and contributor(s) and not of MDPI and/or the editor(s). MDPI and/or the editor(s) disclaim responsibility for any injury to people or property resulting from any ideas, methods, instructions or products referred to in the content.